RERTR 2008 - 30th INTERNATIONAL MEETING ON REDUCED ENRICHMENT FOR RESEARCH AND TEST REACTORS

October 5-9, 2008
Hamilton Crowne Plaza Hotel
Washington, D.C. USA

SMALL-SCALE SPECIMEN TESTING OF MONOLITHIC U-Mo FUEL FOILS

Ramprashad Prabhakaran[a,b], Douglas E. Burkes[a], Daniel M. Wachs[a], James I. Cole[a]
[a]Nuclear Fuels and Materials Division
Idaho National Laboratory, PO Box 1625, Idaho Falls, Idaho 83415-6188, USA

and

Indrajit Charit[b]
[b]Department of Materials Science and Engineering
University of Idaho, Moscow, Idaho 83844-3024, USA

ABSTRACT

The objective of this investigation is to develop a shear punch testing (SPT) procedure and standardize it to evaluate the mechanical properties of irradiated fuels in a hot-cell so that the tensile behavior can be predicted using small volumes of material and at greatly reduced irradiation costs. This is highly important in the development of low-enriched uranium fuels for nuclear research and test reactors. The load-displacement data obtained using SPT can be interpreted in terms of and correlated with uniaxial mechanical properties. In order to establish a correlation between SPT and tensile data, sub-size tensile and microhardness testing were performed on U-Mo alloys. In addition, efforts are ongoing to understand the effect of test parameters (such as specimen thickness, surface finish, punch-die clearance, crosshead velocity and carbon content) on the measured mechanical properties, in order to rationalize the technique, prior to employing it on a material of unknown strength.

1. Introduction

The Reduced Enrichment for Research and Test Reactors (RERTR) program was initiated to develop new nuclear fuels to enable research and test reactors to use low-enriched uranium (LEU) fuels instead of high enriched uranium (HEU) fuels, without significant loss in performance [1]. It is not possible to convert high power research reactors with standard dispersion fuels [2]. Hence, a new monolithic fuel type that possesses the greatest possible uranium density in the fuel region is being developed, where the fuel region consists of a single foil encased inside aluminum (Al) cladding, as shown in Figure 1. Hot-isostatic pressing and friction stir welding are currently being investigated to encapsulate fuel foils in Al alloy

cladding. Material properties of foil are significantly affected by the fabrication techniques. Fabrication methods such as the type of rolling process and annealing method are currently being studied.

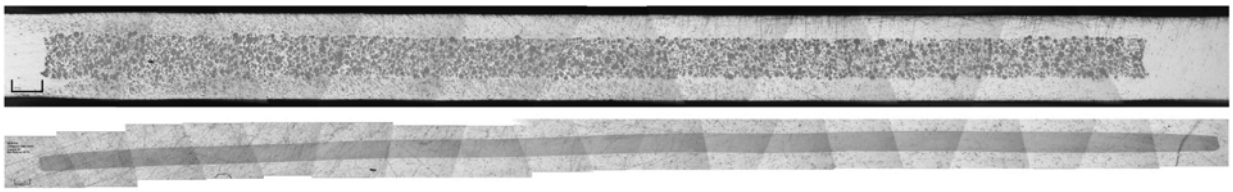

Figure 1: Sample metallographs of a typical Dispersion type fuel plate (top) and Monolithic type fuel plate (bottom)

Mechanical properties of the fuel have a secondary impact on fuel behavior in terms of irradiation. However, mechanical properties of the fuel are extremely important for overall plate properties. In the case of dispersion fuel types, the matrix containing the fuel particles dominates the overall plate mechanical behavior, whereas for plates containing a monolithic alloy, the properties of the foil dominate the overall plate mechanical behavior and failure mode [3]. Understanding this behavior is critical for post-processing operations, such as forming the plates into arced shapes and to study the potential failure modes during irradiation.

1.1 Uranium-Molybdenum (U-Mo) Alloys

Uranium has some limitations, such as poor oxidation and corrosion resistance, low hardness and yield strength, and lack of dimensional stability of the room temperature α phase. Dimensional stability of the fuel during reactor operation is a key issue to be addressed. Thus, the high temperature γ phase is desired based on isotropy that can be retained at room temperature and better resistance to radiation damage [4]. In order to stabilize the high temperature γ phase, an addition of alloying element is needed, such as molybdenum that has a high solid solubility in bcc γ-uranium [2]. Alloys containing 5.4 to 20 wt% Mo (the solid solubility limit of Mo in γ-U) retain the γ phase at room temperature [5]. Alloying above 8 wt% Mo has little effect on fuels for low burn-up applications; however, it shows significant improvements in swelling resistance for higher burn-up applications [6]. Swelling resistance, mechanical properties and oxidation resistance of uranium are improved by increased Mo alloying additions.

Uranium-Molybdenum (U-Mo) is the fuel of choice for conversion of high-power research reactors due to improved irradiation stability, mechanical properties and oxidation resistance. Six monolithic foil alloy compositions (DU-7Mo, DU-8Mo, DU-9Mo, DU-10Mo, DU-11Mo and DU-12Mo - nominal weight percentages) of depleted uranium (U^{238}, <0.3% U^{235}) and Mo are currently being investigated. Depleted uranium metal feedstock and molybdenum foil were alloyed with a single arc furnace. Monolithic fuel foils were obtained by hot rolling at 650°C. Once the desired foil thickness of approximately 254 μm was achieved, foils were placed back into the box furnace for a final annealing step at 650°C for 120 minutes. Additional information on processing of the monolithic foils can be found in Ref [7].

2. Small-Scale Specimen Testing

The objective of this investigation is to obtain mechanical property information using a greatly reduced volume of material. This is highly important in the development of low-enriched uranium fuels for nuclear research and test reactors, due to the higher irradiation costs, limited neutron irradiation space and need to test and qualify a broad range of processing parameters. Thus, a small-scale mechanical testing capability is essential.

2.1 Shear Punch Testing

Shear punch testing (SPT) has thus far only been carried out on a few cladding/structural materials [8,9] and hence, the intent of the current work is to study the mechanical behavior of fuels and also to develop a standardized SPT procedure and evaluate the mechanical properties of irradiated fuels in a hot cell so that the tensile behavior can be predicted in a number of metallurgical conditions.

SPT is based on blanking a circular disk from a sheet metal specimen [10]. The SPT is a relatively straightforward test that uses a cylindrical punch with a flat end to punch a hole in a thin cylindrical disk with a diameter of 3 mm and thickness (t) of ~ 250 μm. SPT utilizes an INSTRON test frame for applying load with a constant crosshead speed. The load and displacement data are acquired through a data acquisition system. SPT can be performed on a wide variety of materials and also on irradiated conditions. The deformation and failure processes that occur during SPT are analogous to those which occur in uniaxial tension. The load-displacement data can be interpreted in terms of and correlated with uniaxial mechanical properties data (such as yield strength and ultimate tensile strength). SPT can also provide ductility information in addition to strength information [8,11]. Furthermore, SPT is less sensitive to material microstructure and specimen preparation procedure.

The SPT fixture consists of an upper and lower die with hardened steel bushing, as shown in Figure 2. The center holes in the bushing are aligned in both dies. The dies are fit together by a set of alignment pins. The sample of diameter 3 mm is placed at the center between the holes. A flat cylindrical punch of diameter about 1 mm is placed on the sample, to a punch a circular disk from the sample of diameter 3 mm. The force on the punch can be monitored as a function of punch travel.

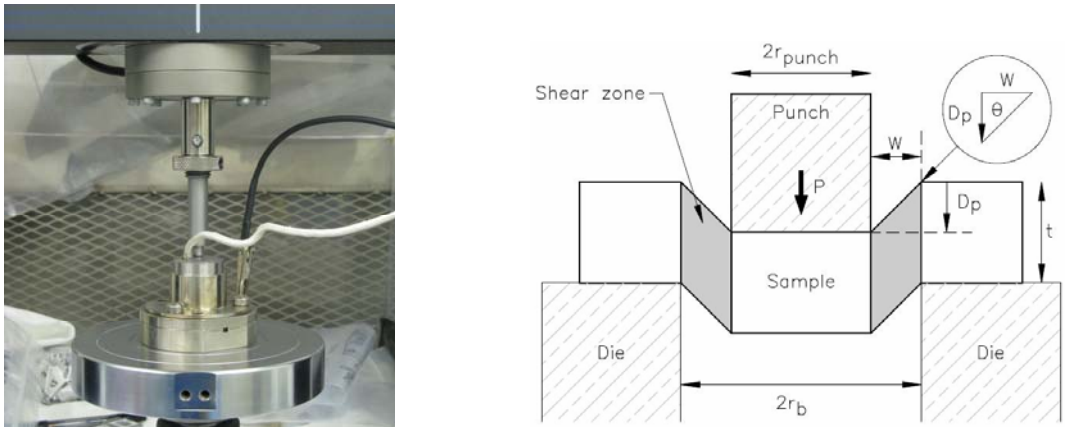

Figure 2: SPT Fixture

The nature of the load-displacement data is a function of the punch-die geometry, particularly the punch profile and punch-die tolerance. To obtain reproducible load-displacement curves for analysis, alignment of the apparatus is critical. The point of deviation from linearity is of major interest and to obtain a distinguishable linear region from which the deviation is recognizable, it is essential that the initial punch penetration of specimens be uniform around the punch circumference. This requires that the punch be exactly perpendicular to the specimen.

2.2 Sub-Size Tensile Testing

Tension tests provide information on the strength and ductility of materials under uni-axial tensile stresses. The tensile test specimens were prepared by placing a section of the foil in a hardened carbon steel punch and die set, ultimately producing a dog-bone specimen. Dimensions of the tensile test specimens are outlined in Figure 3.

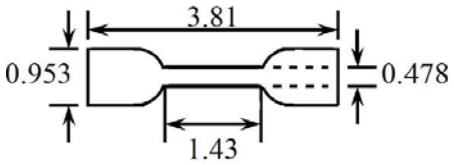

Figure 3: Tensile Specimen Geometry and Dimensions

An Instron 3366 universal testing machine was employed to perform tensile tests at room temperature with a strain rate of 5.83×10^{-4} s^{-1}. A total of at least five specimens were analyzed for each alloy. Engineering stress (σ)-engineering strain (ε) diagrams were constructed from load (P)-displacement (δ) data. Ultimate tensile strength (σ_u) was calculated from the σ-ε data, while a chord method was employed to determine the Young's modulus (E_t) from the linear portion of the σ-ε diagrams. Yield strength (σ_y) was determined using a 0.2% offset. Percent elongation of the samples (e_f) was determined from displacement data at failure and the initial sample length.

2.3. Microindentation Hardness Testing

Hardness, though empirical in nature, can be correlated to tensile strength for many metals. Microhardness test was performed using a Vickers indenter, which is a square-based, pyramidal-shaped diamond indenter with face angles of 136°.

Specimen preparation was performed in accordance with ASTM Standard E3-01 [12]. Specimens for microhardness testing and metallographic studies were cut from the foil and cold-mounted in both the transverse and longitudinal directions. For microhardness studies, the samples were ground and polished to 6 μm surface finish for each alloy. Vickers microhardness measurements were carried out using a LECO LM 100 microhardness tester in each direction (longitudinal and transverse) across the foil cross section at room temperature with a 100 and 500 g_f load and a 15 second dwell time, according to the ASTM Standard E384-06 [13]. The minimum spacing between the indents was kept at least 2.5 times the Vickers diagonal. At least eight readings were taken for each alloy.

2.4. Metallography

Cold mounts containing foils in the longitudinal and transverse directions were ground and polished to a 0.25 μm surface finish for each alloy. For optical metallography, mounts were etched with a solution of 70% phosphoric acid, 25% sulfuric acid and 5% nitric acid with times ranging from 45-150 seconds, depending on alloy compositions.

3. Results and Discussion

3.1 Shear Punch Test Results

The SPT was performed inside the hood on DU-10Mo disks of diameter 3 mm and thicknesses ranging from 150-200 μm. The Figure 4 shows load as a function of displacement for DU-10Mo samples.

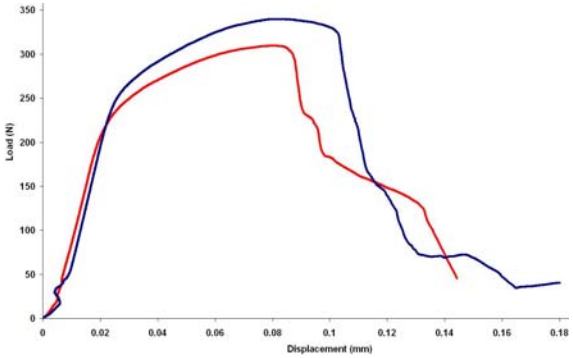

Figure 4: Load versus Displacement curves for DU-10Mo samples

The load-displacement curve obtained using SPT has all the features of a curve produced in a uniaxial tension test. The curve has an initial linear region, a deviation from linearity, a non-linear increase in load with displacement, a load maximum, and a decrease in load with displacement to the point of failure.

The point of deviation from linearity corresponds to permanent penetration of the punch into the specimen. The specimen thins considerably in the region (where the punch tip touches the sample) under both rising and falling load conditions, and finally, the remaining ligament fails catastrophically. The stress state is primarily shear. However, tension and bending contributions are also present. For loads greater than P_y, permanent deformation occurs. Subsequent deformation in the zone is a combination of shear bending and tension with the 'thickness' of the sample continuously decreasing. Apparently, at P_{max}, the decrease in thickness is no longer offset by work hardening in the process zone and the sample deforms and ultimately fails by shear linkage of microvoids under falling load [8].

The yield and maximum loads are taken from the punch load versus displacement data. The shear punch strengths for both yield and maximum conditions can be determined by using the equation: $\tau = P/(2\pi rt)$; where, τ is shear stress; P is load; t is specimen thickness and r is an effective radius, defined as the average of the punch tip radius (r_p) and bore radius (r_b) [8,11].

Shear strain can be calculated by using the equation, $\varepsilon = D_p/W$; where, D_p is the punch displacement and W is the punch-die clearance (r_b - r_p). The Figure 5 shows shear stress as a function of shear strain for DU-10Mo samples.

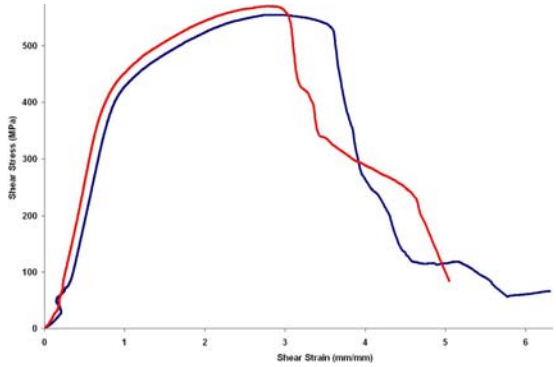

Figure 5: Shear Stress vs. Shear Strain curves for DU-10Mo samples

In order to obtain a correlation between the SPT and tensile data, efforts are ongoing to conduct SPT and tensile testing on materials (calibration materials) with different strength levels (low, medium and high), such as Aluminum 1100, Copper 101, Aluminum 6061, austenitic and martenstic stainless steels. The data will be plotted to obtain a regression line in the form of $\sigma = C\tau + K$, where σ is the uniaxial tensile stress, τ is the shear punch stress, C and K are correlation constants.

Recently, SPT has been performed on 304L stainless steel (one of the calibration materials) sample disks of thicknesses ranging from 220-250 μm. Figure 6 shows load versus displacement and shear stress versus shear strain curves for 304L stainless steel (SS).

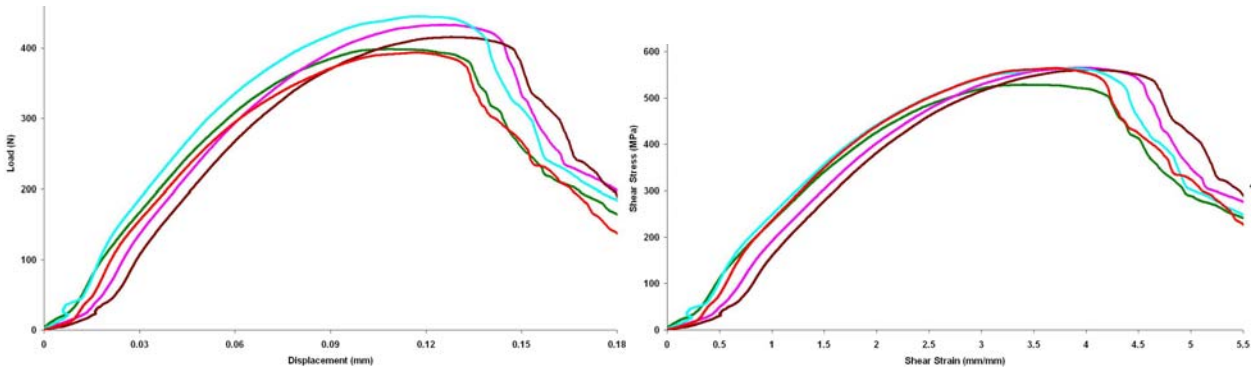

Figure 6: Load vs. Displacement and Shear Stress vs. Shear Strain curves for 304L SS samples

3.2. Sub-Size Tensile Test Results

Subsize tensile testing of DU-(7-12%) Mo alloys revealed that the 0.2% offset yield strength (YS), modulus of elasticity (E) and ultimate tensile strength (UTS) improved linearly with good correlation to increasing molybdenum content, as shown in Figures 7 and 8. The gain in these properties is attributed to the improved resistance to bulk plastic deformation through the increased addition of Mo and associated hardening effect in the γ-phase. The percentage of elongation (% El) does not reveal any clear trend with respect to molybdenum content. In fact,

the % El varied randomly based on where the sample was taken from within the rolled foil, owing both to the notch sensitivity of the rolled alloys and to the variations in carbon impurity [7].

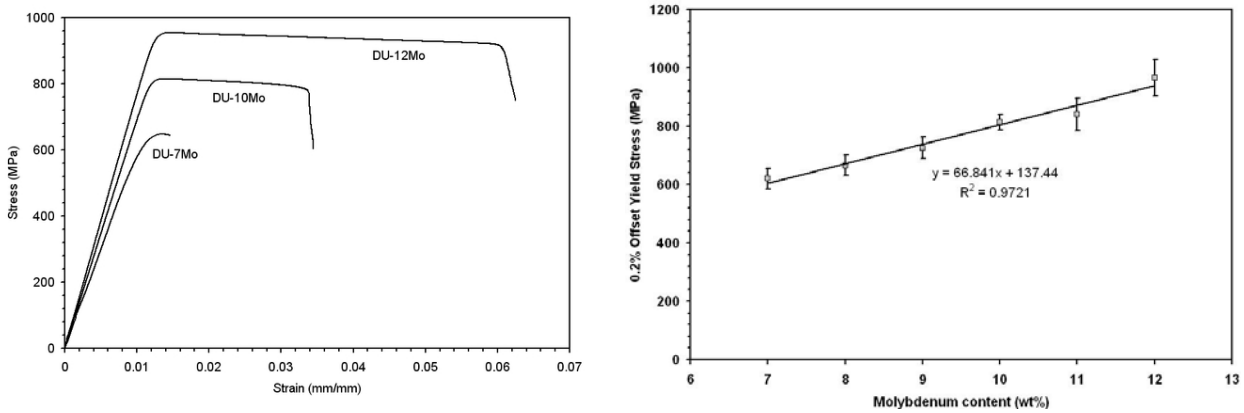

Figure 7: Stress vs. Strain curves and 0.2% offset Yield Strength as a function of Mo content

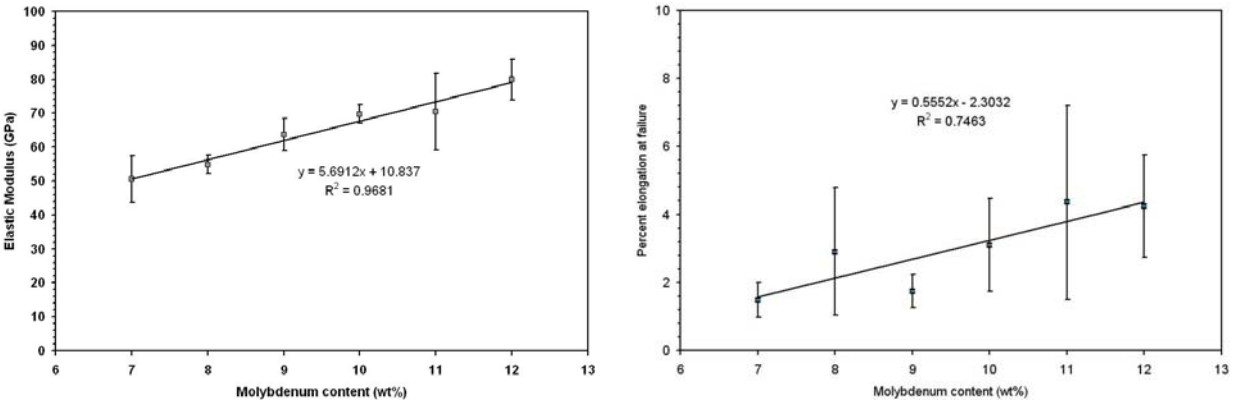

Figure 8: Variation of Elastic Modulus and % Elongation as a function of Mo content

3.3 Optical Metallography and Microhardness Test Results

Optical metallographs of the six DU-Mo alloys studied taken in the longitudinal direction, i.e. parallel with the rolling direction, and in the transverse direction, i.e. perpendicular to the rolling direction, are shown in Figure 9. In each alloy, recovery and recrystallization of the microstructure appears to have occurred upon final rolling and annealing treatment at 650°C for two hours. The grains appeared to be coarser and much more equiaxed in nature for lower Mo contents, with the amount of grain anisotropy increasing with increased Mo contents along with the generation of finer grains. Observation of the optical metallographs revealed the differences in the amount of banding present across the grains that mainly occurred in the central areas of the foil. The darker bands in the images are the Mo rich regions and have a high aspect ratio. It appears that the Mo content has no direct dependence on the amount of banding. The banding effects were relatively random and results from inadequate homogenization of the Mo into the uranium, due to the significant differences in the melt temperature. The inadequate homogenization results in Mo-rich and Mo-lean zones that retain the quenched γ-phase structure [7,14].

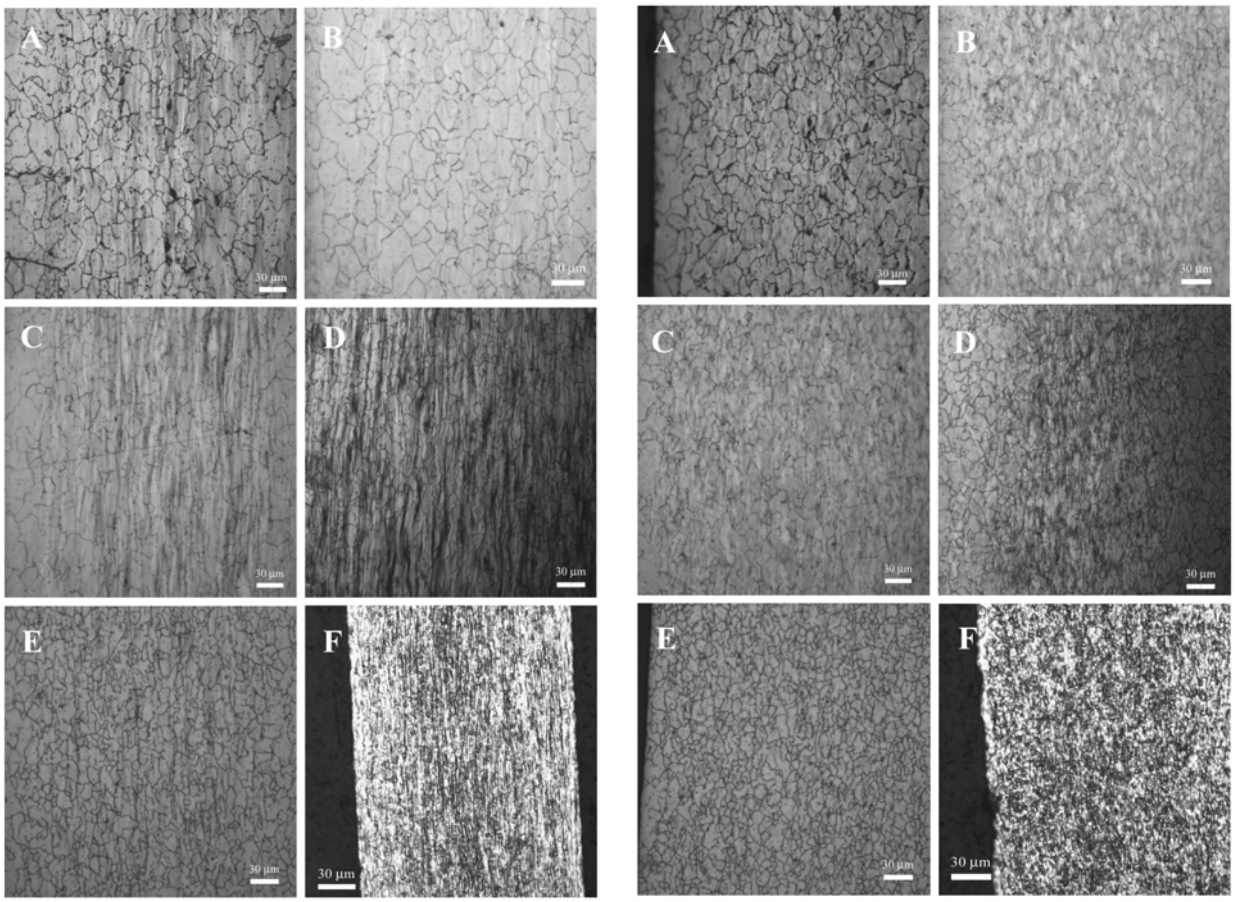

Figure 9: Optical metallographs of DU-Mo alloys (Left: Longitudinal and Right: Transverse)
(A: DU-7Mo, B: DU-8Mo, C: DU-9Mo, D: DU-10Mo, E: DU-11Mo and F: DU-12Mo)

Grain size measurements were also performed, according to the ASTM Standard E112-96, [15] using an Abrams Three-Circle procedure on the six DU-Mo alloys and the results are shown in Figure 10. The relative error for each measurement is less than 10% and is considered to be acceptable precision for most purposes. As expected, the average grain diameter decreased with increased Mo content, especially between 8 and 12 wt% Mo.

Vickers microhardness values (HV) as a function of Mo content clearly showed an increase in the hardness number as the Mo content increased, as shown in Figure 10. The increase in the hardness of DU-Mo alloys results from the solid-solution hardening of the γ-phase with increased Mo content [16,17,18]. The HV increased linearly with exceptional correlation for Mo contents ranging from 8 to 11 wt% Mo (for 100 g_f load). However, both the DU-7 Mo alloy and the DU-12 Mo alloys were slightly above the linear trend. The darker bands in the DU-12Mo metallographs are more closely spaced than the other alloys containing significant banding (DU-7Mo, DU-9Mo, and DU-10Mo). The grain size of DU-12Mo alloy was 9.1 µm. An average diagonal of 23.1 µm (with 100 g_f) was obtained from the hardness testing. Since the diagonal will include a significant portion of the chemical banding (or Mo rich zones), this alloy had higher hardness number. The chemical bands of DU-7 Mo, DU-9Mo, and DU-10Mo alloys had similar aspect ratios, but are more widely spaced than the bands for the DU-12Mo alloy.

Furthermore, the grain size increased with decreased Mo contents, as did the average diagonal of the hardness measurement [7].

The Vickers microhardness test was also performed with 500 g_f load to study the effect of load on hardness values, thus taking into account an increased number of grains and average, rather than just a local measurement. The HV increased linearly with exceptional correlation for Mo contents ranging from 7 to 12 wt% Mo (for 500 g_f load). An average diagonal of 52 µm (with 500 g_f) was obtained for DU-12Mo. This observation shows the sensitivity of the hardness measurement to both local composition and indenter load.

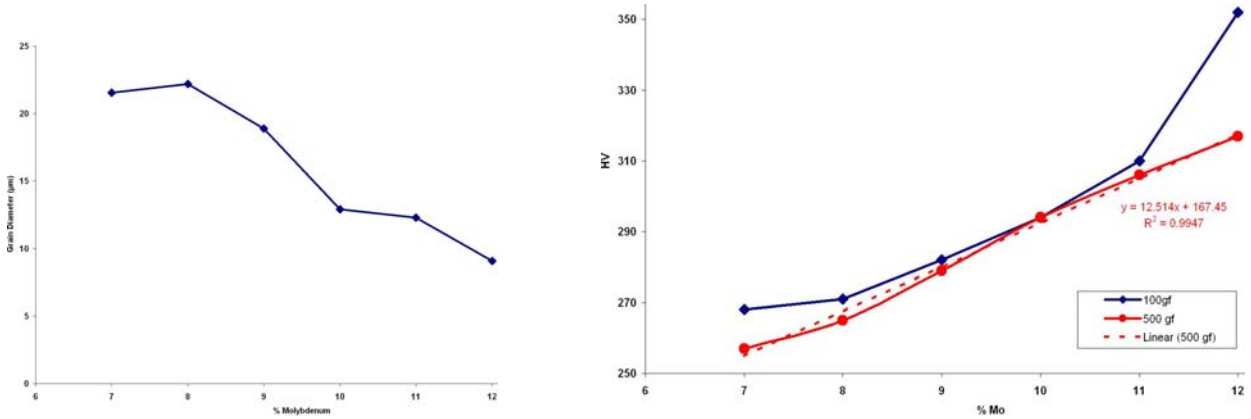

Figure 10: Average Grain Diameters and Vickers Hardness values as a function of Mo content

4. Future Work

Additional SPT testing is being performed on the remaining calibration materials and DU-(7-12%) Mo alloys, in order to obtain correlation constants. Efforts are also ongoing to understand the effect of test parameters (such as specimen thickness, surface finish, punch-die clearance, crosshead speed and carbon content) on the measured mechanical properties and to rationalize the technique, prior to employing it on a material of unknown strength. Once the SPT procedure is standardized, the setup will be installed in a hot-cell for evaluation of irradiated fuel materials.

5. Acknowledgements

This work is supported by the U.S. Department of Energy (DOE) and Office of the National Nuclear Security Administration (NNSA), under DOE Idaho Operations Office Contract DE-AC07-05ID14517.

6. References

[1] J. L. Snelgrove, G. L. Hofman, M. K. Meyer, C. L. Trybus and T. C. Wiencek, Nuclear Engineering and Design, Vol. 178 (1997) 119.
[2] A. N. Holden, Dispersion Fuel Elements, Gordon and Breach Science (1968).

[3] D. E. Burkes, D. M. Wachs, D. D. Keiser, J.-F. Jue, J. Gan, F. J. Rice, R. Prabhakaran, B. Miller and M. Okuniewski, "Fresh Fuel Characterization of U-Mo Alloys," Proceedings of the 30th International Meeting on Reduced Enrichment for Research and Test Reactors, Washington, D.C., October 5-19, 2008.
[4] J. H. Kittel, B. R. T. Frost, J. P. Mustelier, K. Q. Bagley, G. C. Crittenden and J. Van Dievoet, Journal of Nuclear Materials, Vol. 204 (1993) 1.
[5] P. E. Repas, et al., AMRA/CR-63-02/1F (1963).
[6] G. Beghi, EURATOM EUR 4053 e (1968).
[7] D. E. Burkes, R. Prabhakaran, J-F Jue and F. J. Rice, submitted to Metallurgical and Materials Transactions A, as a full length article April 2008.
[8] G. E. Lucas, Journal of Nuclear Materials, Vol. 117 (1983) 327.
[9] M. B. Toloczko, R. J. Kurtz, A. Hasegawa and K. Abe, Journal of Nuclear Materials, Vol. 307-311 (2002) 1619.
[10] T. M. Chang and H. W. Swift, Japan Institute of Metals, Vol. 78 (1950) 119.
[11] G. E. Lucas, et al., ASTM STP 888 (1986) 112.
[12] ASTM E3-01, "Standard Guide for Preparation of Metallographic Specimens," ASM International, West Conshohocken, PA (2004).
[13] ASTM E384-06, "Standard Test Method for Microindentation Hardness of Materials," ASM International, West Conshohocken, PA (2004).
[14] D. E. Burkes, T. Hartmann, R. Prabhakaran and J-F. Jue, submitted to Journal of Alloys and Compounds as a full length article in June 2008.
[15] ASTM E112-96, "Standard Test Methods for Determining Average Grain Size," ASM International, West Conshohocken, PA (2004).
[16] R. F. Hills, et al., Journal of Nuclear Materials, Vol. 11 (1964) 149.
[17] M. B. Waldron, et al., AERE-M/B-2554 (1958).
[18] P. Pascal, ed., Nouveau Traite de chimie minerale - Tome XV, quatrieme fascicule, Paris (1960) 377.